Pak. J. Bot., 55(1): 171-184, 2023. DOI: http://dx.doi.org/10.30848/PJB2023-1(20)

LACK OF PHYLOGEOGRAPHIC PATTERN IN POPULATIONS OF *DACRYCARPUS IMBRICATUS* (PODOCARPACEAE) FROM MAINLAND CHINA AND HAINAN ISLAND

YANG PENG[1], FENG DENG[1], LI LIU[1], CAN CUI[1], ZHEN WANG[1], NING LI[1], YINGJUAN SU[1,2*] AND TING WANG[2,3*]

[1]*School of Life Sciences, Sun Yat-sen University, Guangzhou 510275, China*
[2]*Research Institute of Sun Yat-sen University in Shenzhen, Shenzhen 518057, China*
[3]*College of Life Sciences, South China Agricultural University, Guangzhou 510642, China*
[*]*Corresponding author's email: suyj@mail.sysu.edu.cn, tingwang@scau.edu.cn*

Abstract

Historical climate fluctuations and geological events can affect the distribution range and demographic history of plant populations. *Dacrycarpus imbricatus* is a member of the Podocarpaceae family, mainly distributed in mainland China and Hainan Island in China. It thus provides a framework for unraveling the specific impact of Qiongzhou Strait on the phylogeographic pattern of the species. In this study, seven populations were sampled throughout its distribution range in China. Based on the variation of chloroplast DNA (cpDNA), the *trnF-L* noncoding region sequence, phylogeographic pattern, population genetic structure, population history, and ecological niche model of *D. imbricatus* were calculated. The haplotype diversity was 0.719, and the nucleotide diversity was 1.630×10^{-3}. Moreover, the results did not show a significant phylogeographic pattern between the island and the mainland populations. Qiongzhou Strait did not serve as a geographic barrier in genetic variation. The haplotype network diagram and a mismatch distribution indicated that the *D. imbricatus* population had experienced a population expansion event. Ecological niche modeling suggested the distribution range of *D. imbricatus* population has gradually expanded northward. These results might contribute to establishing ecological reserves and understanding the impact of Qiongzhou Strait on plants in coastal areas of East Asia.

Key words: *Dacrycarpus imbricatus*; Phylogeography; Hainan Island; Mainland China; Qiongzhou Strait.

Introduction

Dacrycarpus imbricatus (Blume) de Laub., (Podocarpaceae), an evergreen tree, can reach up to 40 meters (de Laubenfels, 1988). The habitat for the species is generally valleys in mountain forests with slightly acidic soil pH at an altitude of about 400 to 1,500 meters. Its seeds are oval and lustrous and wrapped in a fleshy red arbor when they are mature. *Dacrycarpus imbricatus* is mainly distributed in tropical areas, while a little grows in subtropical regions. In China, the habitat of *D. imbricatus* is mainly located in Hainan Island, Guangxi, Yunnan, and Guangdong (Fu *et al*., 1999; Su *et al*., 2010). In addition, the species has been found in Indonesia, Vietnam, Cambodia, Myanmar, and Laos (Wilf, 2012; Thomas *et al*., 2007). *D. imbricatus* has a long life span, which is beneficial for maintaining the population's high genetic variation (Varvio *et al*., 1986; Maki & Morita, 1998). Molecular and fossil evidence indicate that the minimum divergence time of *Dacrydium* was 54 Ma (million years) ago (Quiroga *et al*., 2016). In addition, the complete chloroplast genome of *D. imbricatus* is 133,816 bp in length (Li, 2019). The chromosome karyotype of the species is 2n = 20 = 16 M + 4 SM (Zhou & Gu, 2001).

Climate change and geographical events have crucial effects on species richness, population structure, and genetic diversity (Liu *et al*., 2020; Kissling *et al*., 2012). The biogeographic pattern of the *Podocarpus* clades is related to paleoclimatic changes (Quiroga *et al*., 2016). Climate change has a significant impact on the range of plant species. In addition, species on islands are prone to differentiation due to isolation and heterogeneous habitat conditions (Chiang *et al*., 2006). Therefore, species with mainland distributions are generally considered to be a good model to explore the isolation and are vital research objects in phylogeography (Chiang *et al*., 2006). The Qiongzhou Strait, one of the three major straits in China, with an average width of 30 kilometers, is a deep narrow channel between mainland China and Hainan Island (Shi *et al*., 2002; Chen *et al*., 2009; Zhu *et al*., 2014; Bai *et al*., 2020). Thus, studying the phylogeography of the species living on mainland and the island helps reveal the relationship between geographical events and population genetic variation.

Generally, a strait or sea between an island and the mainland is thought to contribute to genetic diversification and speciation. The Western Cretan Strait had a significant impact on the genetic divergence of *Nigella Arvensis* (Jaros *et al*., 2018). Population genetics studies based on *Ilex integra* show that geographical isolation between the mainland and the island reduced gene exchange between populations (Leng *et al*., 2005). Su *et al*., (2005) analyzed the genetic differentiation and phylogeography of *Alsophila spinulosa* population, suggesting that the Qiongzhou Strait between Hainan Island and Guangxi had blocked the gene exchange between the populations. However, the emergence of land bridges provided conditions for the spread of populations between the islands and the mainland, such as *Acmispon dendroideus* var. *traskiae* (Wallace *et al*., 2017), *Quercus variabilis* (Chen *et al*., 2012), *Pinus luchuensis* (Chiang *et al*., 2006). Although South China was not directly affected by the Quaternary Ice Age, frequent climatic shifts have resulted in sea-level changes with the submergence of land bridges between the mainland and the island; this had a profound impact on the biological communities in this region (Hewitt, 2000, 2004; Parker *et al*., 2006; Liu *et al*., 2020).

In this study, phylogeographic patterns and genetic structure of *D. imbricatus* in South China were assessed by molecular variance, ancestral area reconstruction, Approximate Bayesian Computation, and ecological niche modeling, based on the *trnF-L* noncoding region of

chloroplast DNA (cpDNA). The major goals were (i) to analyze whether the divergence of *D. imbricatus* between mainland China and Hainan Island was consistent with the time of formation of Qiongzhou Strait; (ii) to explore the specific impact of the formation of Qiongzhou Strait on the genetic differentiation of *D. imbricatus* in China, and (iii) to unravel the influence of climate change on the current distribution pattern of *D. imbricatus*.

Methods

Plant material and DNA extraction: A total of 85 *D. imbricatus* individuals were collected from seven populations in South China. Three populations were from the mainland China, including Dinghushan (DH), Liuxiangxiang (LX), and Nanshahe (NS), while four populations were sampled on Hainan Island, located at Diaoluoshan (DLS), Bawangling (BWL), Jianfengling (JFL) and Wuzhishan (WZ), respectively (Table 1 and Fig. 1). Fresh leaves of all individuals were stored with silica gel until DNA isolation. The modified cetyltrimethyl ammonium bromide (CTAB) protocol was used to extract the total genomic DNA (Su *et al*., 2005).

PCR amplification and sequencing: The primers *trnF* (5′-ATT TGA ACT GGT GAC AGG AG-3′) and *trnL* (5′-CGA ATT CGG TAG ACG CTA CG-3′) (Taberlet *et al*., 1991) were used to amplify the cpDNA *trnF-L* noncoding sequences. The PCR reaction volume was 50 µL. The thermocycling profile consisted of 5 min at 94°C, 30 cycles of 45 s at 94°C, 50 s at 55°C, 80 s at 72°C, and an additional extension for 10 min at 72°C. One percent (1%) agarose gel electrophoresis was used to separate and purify the PCR product and then ligate the purified PCR product to pMD18-T vector. They were used to transform competent *Escherichia coli* cells DH-5α. In addition, to identify the positive clones, blue/white selection and PCR amplification were performed. Purified plasmid DNA with primers M13F and M13R was sequenced in both directions by standard methods on an ABI 377 automated sequencer.

Genetic diversity and population structure analysis: GenBank accession numbers of the determined *trnF-L* noncoding sequences of haplotypes were MW004857-MW004889, respectively. Chloroplast sequences of *trnF-L* were aligned in BioEdit v7.0.9 (Hall, 1999), and then adjusted manually. The haplotype content, haplotype diversity (*Hd*), nucleotide diversity (π) for the species and each population, differentiation coefficient (*G*st), and population migration number (*Nm*) were estimated using DnaSP v5.0 (Librado & Rozas, 2009). A haplotype geographic distribution map was drawn by DnaSP v5.0 based on the distribution of the haplotype in each population. A haplotype network was created by Network v5.0.1.1 (Fluxus Technology Ltd.) to further investigate the relationships among unique haplotypes. AMOVA (molecular variance) and Hierarchical AMOVAs in Arlequin v3.5 (Excoffier & Lischer, 2010) were employed to conduct the genetic structure. Ten thousand permutations were used to test the significance of the estimated fixation. In addition, to analyzing whether there was significant genetic differentiation among geographic populations, the genetic differentiation (*F*st) matrix between two populations and the geographical distance matrix were combined to perform the Mantel's permutation test (10,000 permutations) (Mantel, 1967).

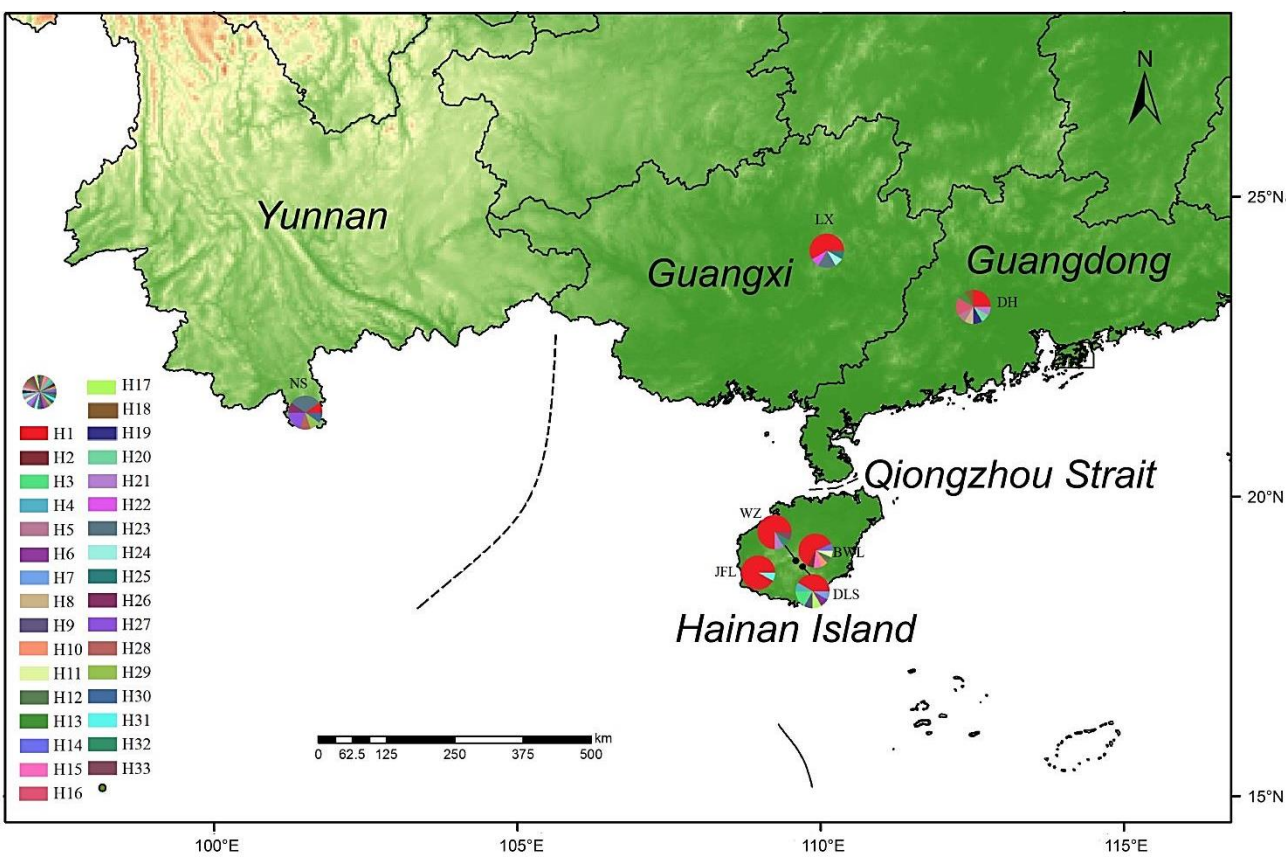

Fig. 1. Sampling locations, distribution of haplotypes and barrier between *Dacrycarpus imbricatus* populations (black dotted line).

Table 1. Details of sample sizes, sample locations (longitude and latitude), number of haplotypes and genetic diversity for *Dacrycarpus imbricatus*.

Populations	Sample sizes	Locations	Longitude (E)	Latitude (N)	Number of haplotypes	Haplotype diversity (*Hd*)	Nucleotide diversity (π)
DH	12	Guangdong	112°31'	23°10'	9	0.939	0.00274
LX	12	Guangxi	110°06'	24°06'	5	0.667	0.00110
NS	10	Yunnan	101°30'	21°24'	7	0.911	0.00275
DLS	12	Hainan	109°52'	18°50'	7	0.833	0.00198
BWL	15	Hainan	109°55'	19°6'	7	0.657	0.00136
JFL	12	Hainan	108°58'	18°44'	2	0.167	0.00019
WZ	12	Hainan	109°44'	18°54'	4	0.455	0.00057
Total	85				33	0.719	0.00163

Demographic history analysis: Pairwise mismatch distribution analyses were performed using DnaSP v5.0 to evaluate whether the populations had experienced a recent range expansion. One thousand bootstrap resamplings were set, and the genetic distance was fixed as a pairwise difference. The sum of squared deviations (SSD), Harpending's raggedness index (H_{Rag}), and its *P*-values were also computed to test the significance of the population expansion model (Harpending, 1994). In addition, a neutral test of *trnF-L* noncoding sequences of *D. imbricatus* was conducted by computing Tajima's *D.,* (Tajima, 1989) and Fu and Li's *D** (1993). To investigate the effective population size of *D. imbricatus*, a Bayesian skyline plot (Drummond *et al*., 2005) was obtained by BEAST v1.8.2 (Drummond *et al*., 2012) and Tracer v1.6 (http://beast.community/tracer). Combined with the results of jModeltest v2.1.5 (Darriba *et al*., 2012), the applicable models were sorted and screened to determine the most suitable model with the minimum AIC value. The Markov Chain Monte Carlo (MCMC) was run for 5×10^7 generations, using a burn-in length of 5×10^6, and then sampled at every 5,000 generations. The model of a molecular clock was an "uncorrelated lognormal relaxed clock". Barrier v2.2 (Manni *et al*., 2004) was used to investigate the barriers among *D. imbricatus* populations. Firstly, 100 sets of bootstrap data were obtained from the Seqboot package of Phylip v3.695 (Felsenstein, 1989), and then converted to Arlequin input file format. One to three barriers, based on information about the geographic coordinates (longitude and latitude) were set and the genetic distance matrix of seven populations. The *F*st matrix of seven populations was used as the genetic distance data.

Divergence time estimation: To calculate the divergence time for all haplotypes, the HKY model and UCLN relaxed-clock model of DNA sequence evolution in BEAST V1.8.2 were selected, based on the AIC results of jModeltest V2.1.5. *D. pectinatum*, *Podocarpus henkelii* and *P. forrestii* were selected for the outgroup. Fifty-five Ma (95% HPD: 54.18 to 55.82 Ma) was used to calibrate the root node, which was the most recent common ancestor (MRCA) of *Podocarpus*, *Retrophyllum*, *Dacrycarpus*, *Falcatifolium* and *Acmopyle* (Hill & Carpenter, 1991; Kranitz *et al*., 2014). The MCMC was run for 5×10^7 generations, using a burn-in length of 5×10^6, and then sampled every 5,000 generations.

Ancestral area reconstructions and approximate bayesian computation: According to the geographical distribution of *D. imbricatus*, the seven populations were divided into two groups: mainland China and Hainan Island. The mainland group included populations: NS, LX, and DH, and the Hainan group involved: WZ, JFL, DLS, and BWL. Statistical Dispersal-Vicariance Analysis (S-DIVA), Bayesian Binary MCMC (BBM) analysis, and Statistical Dispersal-Extinction-Cladogenesis (S-DEC) were conducted, which were implemented in Rasp v3.1 (Yu *et al*., 2015), using trees retained from the BEAST analysis. In three models, both binary trees and the number of trees were set at 100,000, and the discard trees were set at 20,000.

To infer the evolutionary history situation of *D. imbricatus*, Approximate Bayesian Computation was employed using DIYABC v2.1.0 (Cornuet *et al*., 2014). Pop1 included three populations (NS, LX, DH); its effective population size was recorded as N1. Pop2, included four populations (WZ, JFL, DLS, BWL), and its effective population size was recorded as N2. The ancestral effective population size was defined as Na. 0 and t1 represented the current and the population divergence generations, respectively. Based on the population history of *D. imbricatus*, three possible scenarios were included in the historical model option (Fig. 2). According to scenario 1, the *D. imbricatus* populations had a common ancestral group, separated into a mainland group (pop1) and a Hainan Island group (pop2) at t1 generations. Scenarios 2 and 3 considered that there was no common ancestral group in the population of *D. imbricatus. S*cenario 2 considered that Pop1 derived from the Hainan group (pop2) at t1 generations, and scenario 3 assumed that the Hainan group (pop2) derived from the mainland group (pop1) at t1 generations. Parameter ranges were set under the historical model, where N1 was 0 to 400,000, N2 was 10 to 50,000, Na was 10 to 1,500,000, and t1 was 10 to 10,000. The mutation model was set as a Hasegawa-Kishino-Yano (HKY) model. According to the online calculation results for PhyML (http://www.atgc-montpellier.fr/phyml), the percentage of invariant sites was set as 0, and the shape of the gama (G value) was set to 99.8230. The interval of the mean mutation rate (useq_1) was 1×10^{-9} to 1×10^{-6}, and the interval of mean

coefficient K_C/T (k1seq_1) was set as 0.050 to 1,000. One sample of summary statistics contained the number of haplotypes (NHA), several segregating sites (NSS), and the private segregating sites (PSS) for all samples. Two sample summary statistics contained the *F*st between all pairs of samples. The generations were run for 3×10^6 in total and 1×10^6 generations per model. Principal Components Analysis (PCA) was used to assess the pre-evaluated scenario-prior combinations analysis. As the number of prior plots per scenario was 1,000, the PCA clustering figure was obtained. Logistic regression analysis was used to choose the suitable model by calculating the posterior probability for each scenario. Among the 3×10^6 operations simulated, 1% of the data set closest to the observed data was selected for analysis. Based on the scenario selected, the data set of the scenario closest to the observed data was chosen to calculate the parameter's posterior distribution.

Ecological niche modeling: To infer distributional changes for *D. imbricatus*, ecological niche modeling (ENMs) was produced in MAXENT v3.3.3k (Phillips *et al*., 2006) for five periods: 2070, current (1950 to 2000), Mid-Holocene (6,000 years ago), last glacial maximum (LGM, 22,000 years ago) and last interglacial (LIG, ~120,000 to 140,000 years ago). The convergence threshold was 10^{-5}, and the default parameter of the reaction number was 500. Among the 57 records, 50 were from the Global Biodiversity Information facility, and the others were from this study. A current distribution model was developed at 2.5 arc-min resolution using nineteen bioclimatic data layers (WorldClim dataset). The Model for Interdisciplinary Research on Climate (MIROC) (Hasumi & Emori, 2004) and the Community Climate System Model (CCSM) (Collins *et al*., 2006) were employed to infer the habitat during the LGM. The models for all distribution predictions were repeated 15 times, and Jackknife analysis was performed in the MAXENT model to find out which environmental variable was most significant for determining the distribution of *D. imbricatus*. To test the accuracy of each model's prediction, the value of the area under the Receiver Operating Characteristic (ROC) Curve (AUC) (Fawcett, 2006) was calculated. A higher AUC value (>0.9) indicates higher accuracy and validity of the model (Swets, 1988). Then, the simulated distribution map was obtained by ArcGIS v10.2 (ESRI, Redlands, CA, USA).

Results

Population genetic diversity analysis: The sequence of *trnF-L* was 910 bp after alignment. Forty-five mutation sites and seven parsimony information sites were detected, and 33 haplotypes from 85 individuals in seven populations were obtained. Most haplotypes were region-specific and were only distributed in a specific area. Except for haplotype H1, which existed in all populations, only haplotypes H21 and H23 were distributed in two different populations (Table 2). Among them, H21 was distributed in Guangdong and Hainan, and H23 was distributed in Guangxi and Yunnan. At the species level, haplotype diversity was 0.719, and nucleotide diversity was 1.630×10^{-3}. At the population level, the DH population located in Guangdong province had the highest level of haplotype diversity (*Hd* = 0.939), followed by the NS population located in Yunnan province with a *Hd* value of 0.911. However, the JFL population in Hainan province contained only two haplotypes H1 and H31, so that population had the lowest level of haplotype diversity, with a *Hd* of only 0.167. In addition, for nucleotide diversity, the NS population was the highest ($\pi = 2.750 \times 10^{-3}$), and the DH population was second ($\pi = 2.740 \times 10^{-3}$), whereas the JFL population was the lowest ($\pi = 1.900 \times 10^{-4}$). Therefore, both the DH and NS populations had high levels of haplotype diversity and nucleotide diversity, and the JFL population had the lowest among all populations studied (Table 1).

The Nei (1973) algorithm was used to calculate *G*st, which was 0.008755 among the haplotype data for populations of *D. imbricatus*, and its *Nm* was 2.61 per generation. The *F*st value of the genetic differentiation of the *D. imbricatus* population was 0.10388 (0.05 <*F*st <0.15), indicating that the degree of differentiation among the populations was moderate.

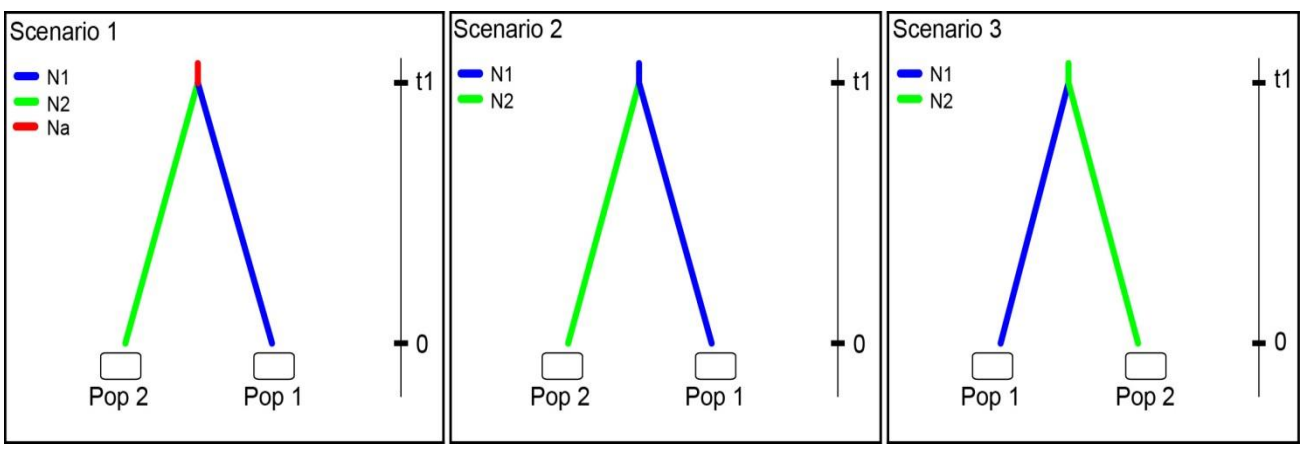

Fig. 2. Scenarios of *Dacrycarpus imbricatus* populations evolutionary history. Blue (N1), green (N2) and red (Na) represented the population size of pop1 (mainland group), pop2 (Hainan Island group) and ancestral group, respectively. 0 and t1 represented the current and the population divergence generations, respectively.

Table 2. Haplotype distribution and number in different *Dacrycarpus imbricatus* populations.

	DLS	BWL	DH	LX	NS	JFL	WZ
H1	5	9	3	7	1	11	9
H2	1						
H3	2						
H4	1						
H5	1						
H6	1						
H7	1						
H8		1					
H9		1					
H10		1					
H11		1					
H12		1					
H13		1					
H14			1				
H15			1				
H16			2				
H17			1				
H18			1				
H19			1				
H20			1				
H21			1				1
H22				1			
H23				2	3		
H24				1			
H25				1			
H26					1		
H27					2		
H28					1		
H29					1		
H30					1		
H31						1	
H32							1
H33							1

Table 3. Coefficient of genetic differentiation (lower left) between populations and geographic distance matrix (upper right) among *Dacrycarpus imbricatus* populations.

	DLS	BWL	DH	LX	NS	JFL	WZ
DLS	0.00000	11543.47	342511.7	201981.2	934385.5	100255.8	15129.25
BWL	0.03197	0.00000	332429.7	191476.6	939357.2	106623.7	21830.19
DH	0.03459	0.06522	0.00000	271685.3	1227618	431858.3	353863.9
LX	0.03371	0.02976	0.07955	0.00000	960586.4	236123.8	201310.5
NS	0.21320	0.29617	0.19634	0.12153	0.00000	834660.4	919342.6
JFL	0.06934	0.00401	0.13636	0.05425	0.38473	0.00000	85492.83
WZ	0.03409	-0.03280	0.04921	0.04167	0.31520	0.06818	0.00000

The genetic differentiation (*F*st) matrix and geographical distance matrix showed that the correlation coefficient *r* was 0.819 (p=0.05), indicating a significant correlation between genetic and geographical distances among populations. The genetic differentiation between the Yunnan population (NS) and the Hainan population (WZ, JFL, BWL, and DLS) was relatively large (Table 3).

The results of AMOVA indicated a lower level of mean genetic differentiation among all the geographic populations of *D. imbricatus;* its percentage among the geographic populations was 11.78% (F_{ST} = 0.118, p<0.01) (Table 4). Within the population, the percentage of genetic differentiation was 88.22%. Hierarchical AMOVA analysis of two geographical locations (Hainan Island and mainland China) based on geographical location was performed, and results indicated that 5.06% (F_{CT} = 0.051) of genetic variation existed between those regions and that 8.68% (F_{SC} = 0.091) genetic variation existed among populations within the regions (Table 4). The AMOVA results showed that the genetic variation mainly occurred in *D. imbricatus* population.

Table 4. Analysis of molecular variance (AMOVA) among or within populations and groups.

Source of variance	d.f.	SS	Variance components	Variance percentage (%)	Fixation indices (p<0.01)
Total					
Among populations	6	21.199	0.18018 Va	11.78	F_{ST} = 0.118
Within population	78	105.283	1.34979 Vb	88.22	
Hierarchical AMOVAs					
Among groups	1	6.208	0.07914 Va	5.06	F_{CT} = 0.051
Among populations within groups	5	14.991	0.13577 Vb	8.68	F_{SC} = 0.091
Within populations	78	105.283	1.34979 Vc	86.27	F_{ST} = 0.137

Notes: d.f, degrees of freedom; SS, sum of squares; F_{CT}, genetic differentiation among groups; F_{SC}, genetic differentiation among populations within groups; F_{ST}, genetic differentiation among populations

Table 5. The neutral test and mismatch distribution analyzes.

	Tajima's *D*	Fu and Li's *D**	Mismatch distribution analyzes	
			SSD **(P_{SSD})**	**H_{Rag} (P_{HRag})**
Total	-2.699 (p<0.001)	-6.661 (p<0.02)	0.073 (0.229)	0.343 (0.297)

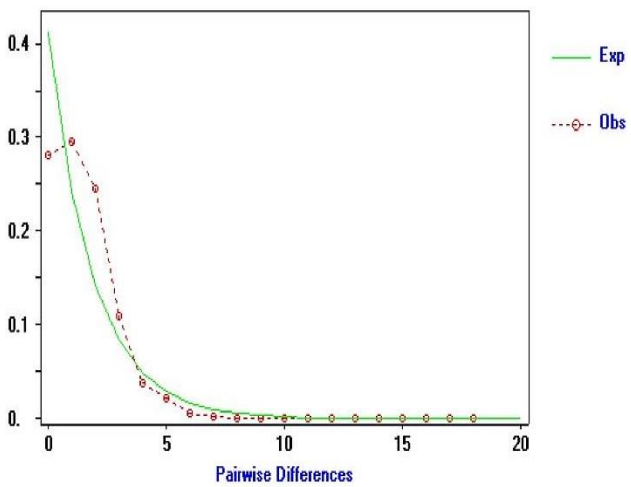

Fig. 3. Mismatch distribution analysis of *Dacrycarpus imbricatus*. The green line and the red dot represented the expected value and the observed value, respectively.

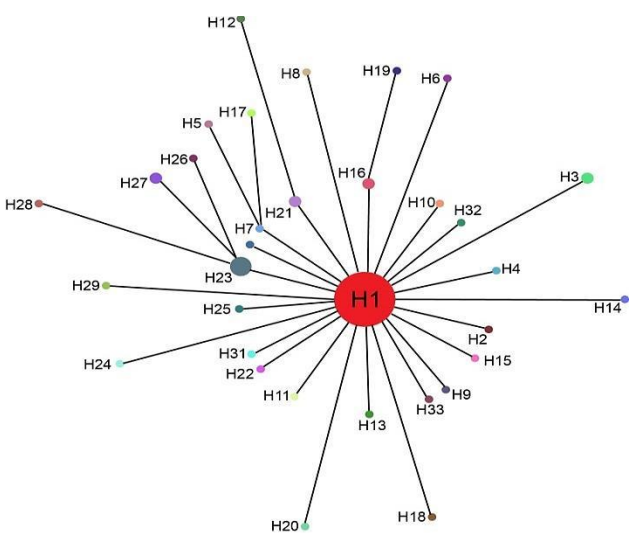

Fig. 4. Network profile. Network of genealogical relationships between the 33 haplotypes found in *Dacrycarpus imbricatus*. Each haplotype was represented by a circle. The sizes of circles were approximately proportional to sample size.

Population expansion and barriers: The mismatch distribution results showed that the sum of squares of dispersion was 0.073 (P_{SSD} = 0.229), and the roughness index was 0.343 (P_{HRag} = 0.297) (Table 5). The mismatch distribution peak diagram presented a single peak (Fig. 3). In the neutral test, Tajima's *D* value and Fu and Li's *D** value were significantly negative, at -2.699 (p<0.001) and -6.661 (p<0.02), respectively. Therefore, both the mismatch distribution and the neutral test results showed that the population of *D. imbricatus* experienced population expansion events.

The haplotype of *D. imbricatus* population showed a star-shaped distribution centered on H1 (Fig. 4), indicating that the *D. imbricatus* population might have experienced population expansion. Furthermore, it was likely that the haplotype H1 was the ancestor that the other haplotypes were derived from. There was a barrier between the NS population and the other six populations in Yunnan (Fig. 1) with a 97% support rate.

Divergence time: The phylogenetic relationship among haplotypes of *D. imbricatus* showed that there was no significant lineage division between the haplotypes from mainland China and Hainan Island. Overall, the divergence time between the different haplotypes of *D. imbricatus* was 21.01 Ma (95% HPD: 37.25 to 7.86 Ma) (Fig. 5).

Bayesian skyline plot analysis of historical demography: The Bayesian skyline plot showed that the population of *D. imbricatus* maintained low but stable and effective population sizes (*Ne*) up to approximately 8 Ma, decreased slowly from 8 to 2.5 Ma, and then increased sharply during the period from 2.5 Ma till now (Fig. 6).

Ancestral area reconstructions and approximate bayesian computation: Under the three models (S-DEC, S-DIVA, and BBM), the ancestral areas of different haplotypes presented a mixed pattern, which indicated the degree of genetic differentiation between the mainland group and the Hainan group was small (Fig. 7).

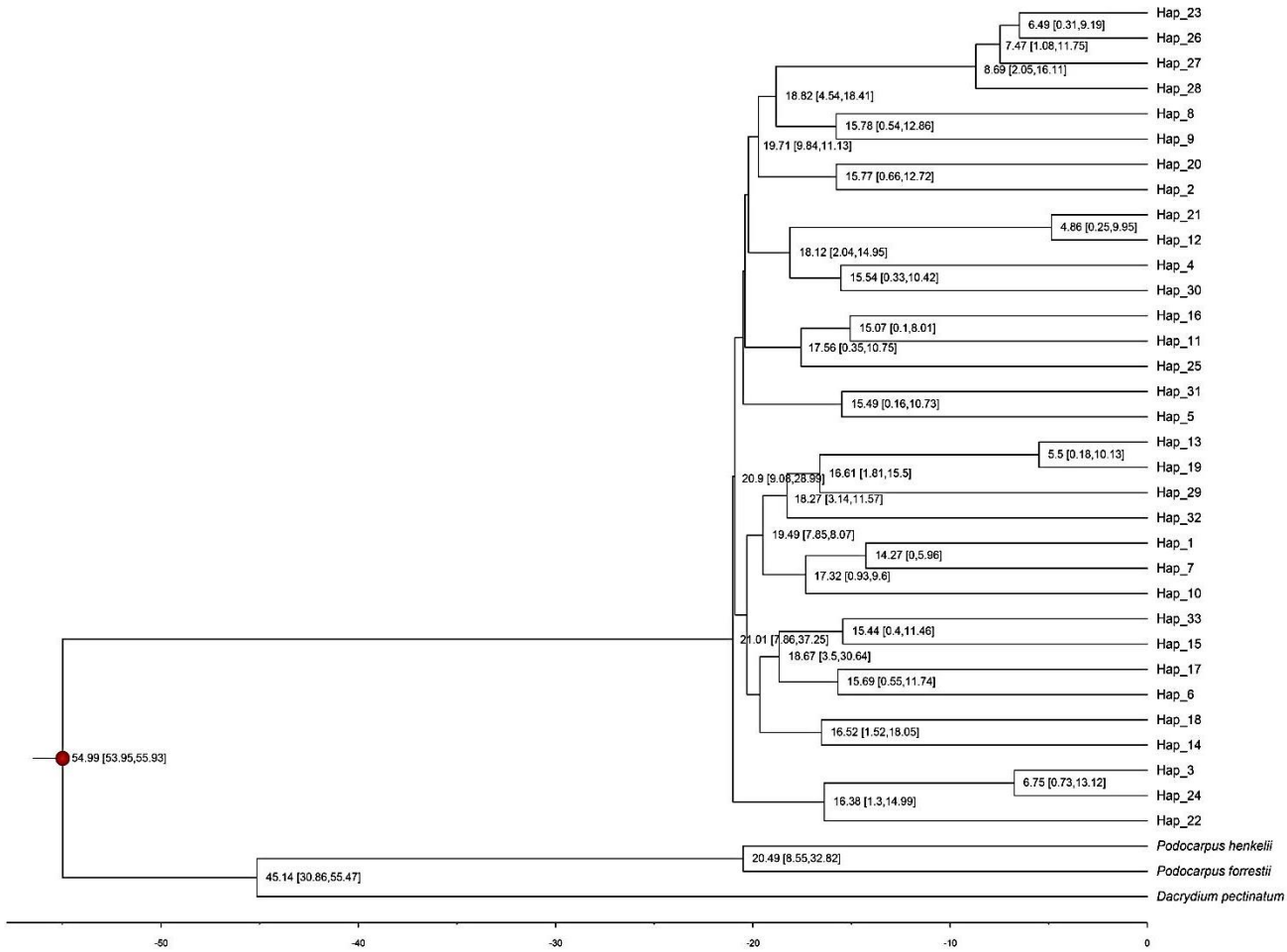

Fig. 5. The divergence time of haplotypes in *Dacrycarpus imbricatus*. The number in square brackets indicated the 95% highest posterior density (HPD). Choosing *Podocarpus henkelii*, *Podocarpus forrestii* and *Dacrydium pectinatum* as the outgroup. The red dot represented the position of the calibration point in the phylogenetic tree.

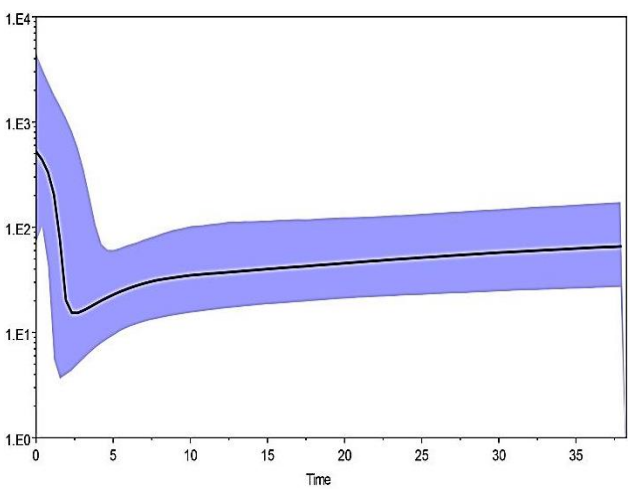

Fig. 6. Bayesian skyline plot of *Dacrycarpus imbricatus*. The unit of x axis was millions of years ago. The y axis represented the effective population size. The solid line inferred the estimates of means, whereas the upper and lower lines delineated the 95% HPD limits.

The PCA cluster diagram suggested high reliability of the parameter setting (Fig. 8). Logistic regression analysis of the situation showed that scenario 1 (green) was the suitable model; namely, the population of *D. imbricatus* had an ancestor group, which was separated into a mainland group (pop1) and Hainan group (pop2) at 1.49×10^4 generations (Fig. 9). A mean generation time of 10 years was assumed for *D. imbricatus* trees; therefore, the ancestor group diverged into the mainland group (pop1) and Hainan group 0.149 Ma. Based on the optimal scenario, the effective population sizes of N1, N2 and Na were 1.90×10^5, 8.13×10^4, and 5.02×10^3, respectively (Table 6). The sum of the effective population sizes of the mainland group and Hainan group was larger than that of their common ancestor. This fact indicated that the population had undergone population expansion.

Ecological niche model: The AUC value for the current potential distribution of *D. imbricatus* was 0.978. Jackknife analysis showed the contribution of different environmental factors used in the model for the distribution of *D. imbricatus* (Fig. 10). When individual climate data were analyzed separately (dark blue), the bio7 (annual temperature range) had the greatest impact on the distribution of *D. imbricatus*. That was followed by bio11 (the coldest average temperature), bio6 (the lowest temperature in the coldest month), and bio4 (seasonal temperature change). The distribution of *D. imbricatus* was apparently closely related to the ambient

temperature. Under the present conditions (1950~2000) (Fig. 11), the predicted distribution of *D. imbricatus* was basically consistent with the actual distribution in mainland China and Hainan Island. Under the MIRCO and CCSM models for the last glacial maximum, the simulated suitable distribution area of *D. imbricatus* was concentrated in Yunnan province. During the LIG, the species was only distributed in southern Yunnan in mainland China. For the Mid-Holocene period, the southernmost part of Guangdong also had a distribution of *D. imbricatus*. The suitable distribution area of *D. imbricatus* has gradually moved northward under present conditions from Hainan Island to the southern coast of mainland China. Furthermore, it was predicted that the distribution range of *D. imbricatus* would be wider in 2070.

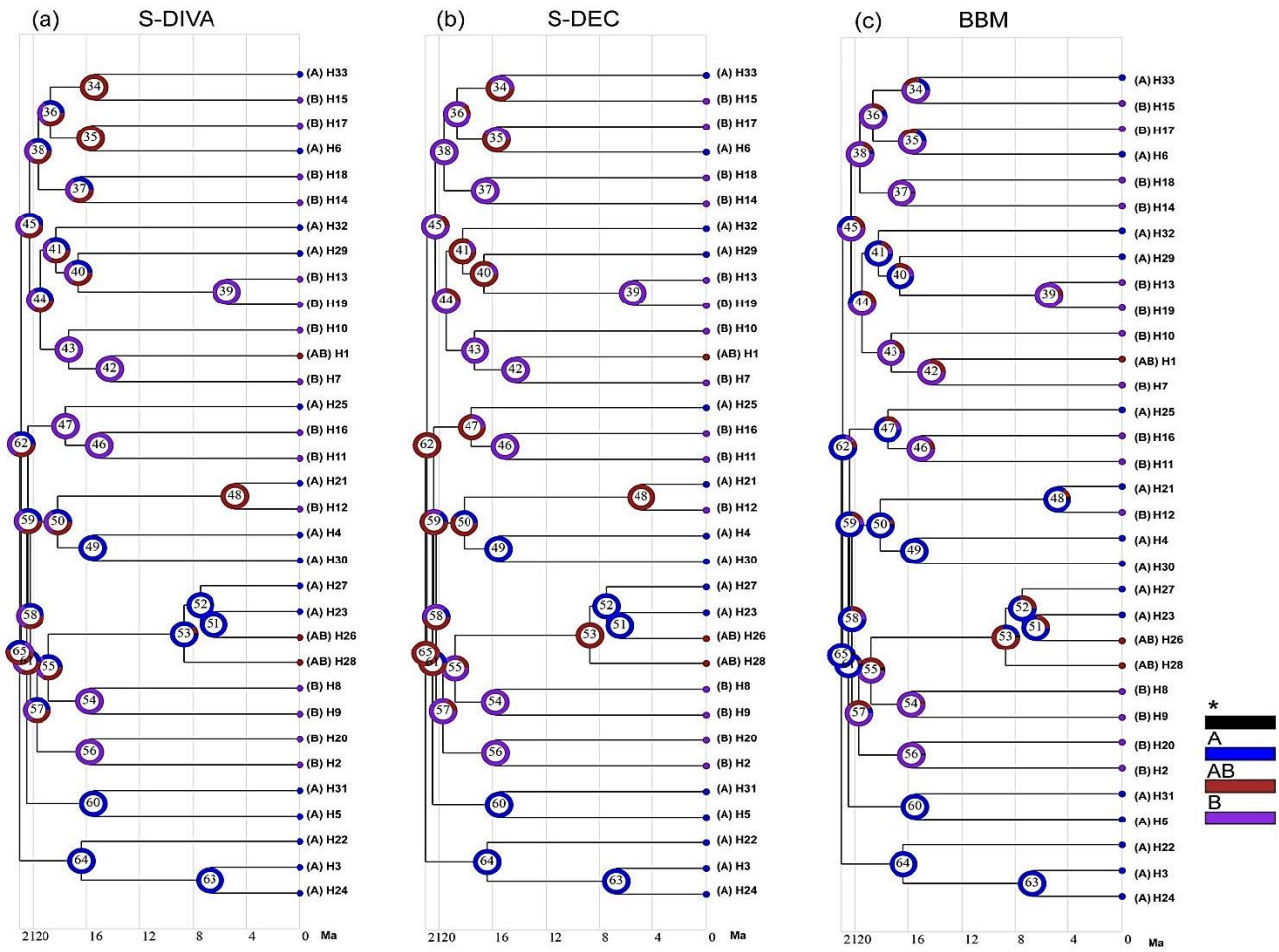

Fig. 7. Ancestral area reconstructions based on (a) S-DIVA, (b) S-DEC, and (c) BBM. Blue, red and purple represented mainland China, the whole region (mainland China and Hainan Island), and Hainan Island, respectively.

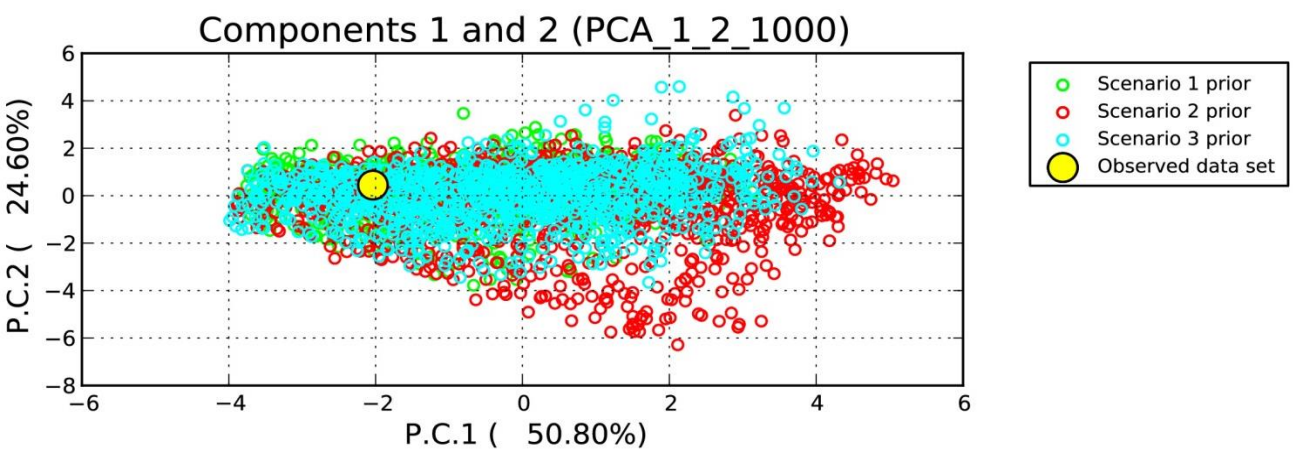

Fig. 8. PCA cluster diagram, in which yellow dots represented observed data set, green, red and blue represented scenario 1 prior, scenario 2 prior and scenario 3 prior, respectively. PC1 represented 50.80% of the total variation, PC2 represented 24.60% of the total variation, and the two components represented 75.4% of the total variation.

Table 6. Model parameter value, including mean, median, mode and 95% confidence interval.

Parameter	mean	median	mode	95% confidence interval
N1	1.99×10^5	1.90×10^5	1.66×10^5	5.86×10^4-3.64×10^5
N2	8.21×10^4	8.13×10^4	7.66×10^4	2.56×10^4-1.40×10^5
Na	4.99×10^3	5.02×10^3	1.43×10^3	5.61×10^2-3.06×10^4
t1	1.49×10^4	1.38×10^4	7.63×10^3	3.33×10^3-9.46×10^3

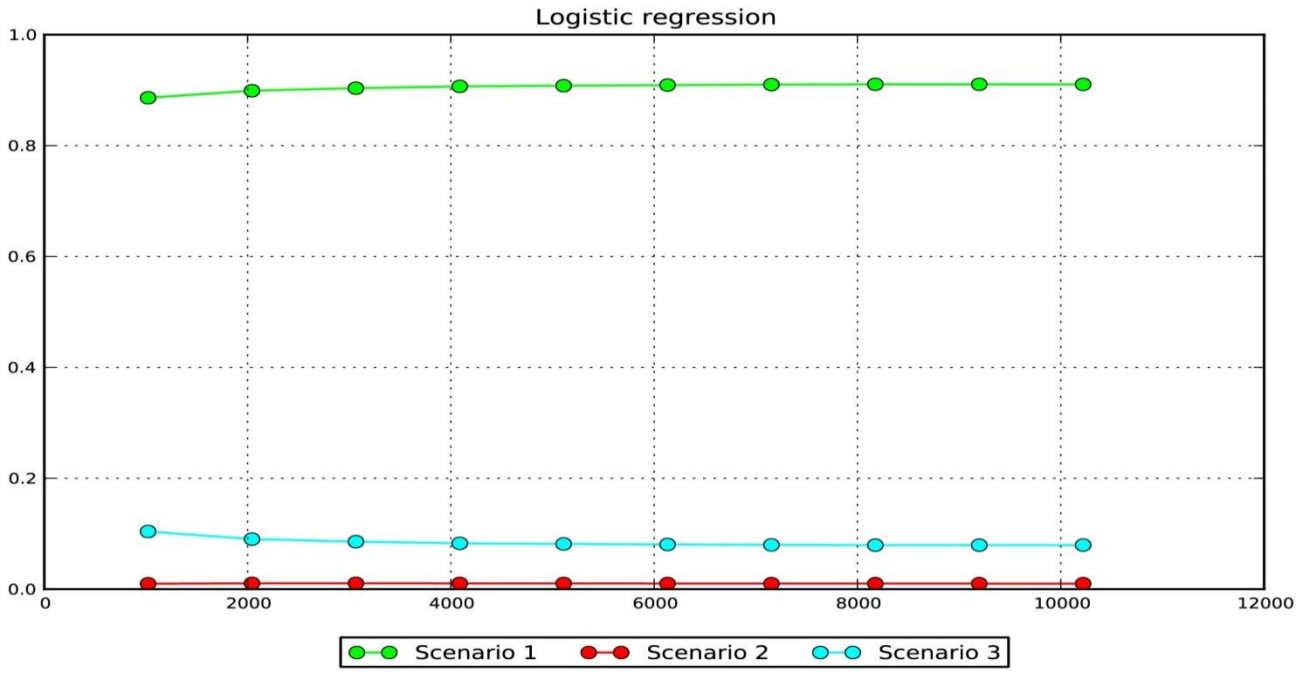

Fig. 9. Logistic regression analysis of the situation. The x axis was the data set. The y axis represented the posterior probability.

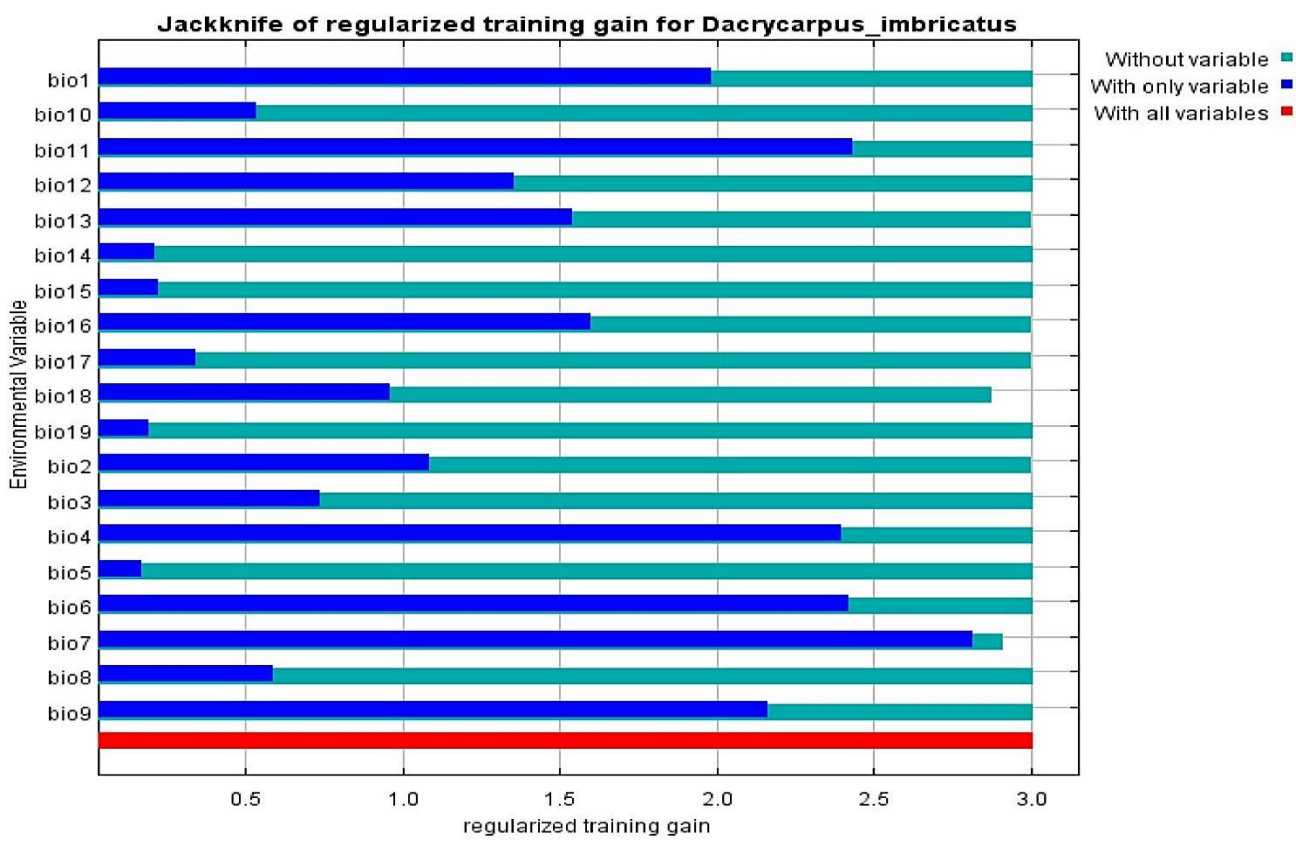

Fig. 10. Jackknife test based on climate variables. Under the three conditions, without variable (green), with only variable (blue) and with all variables (red), the contribution rate of variables to the distribution of *Dacrycarpus imbricatus*.

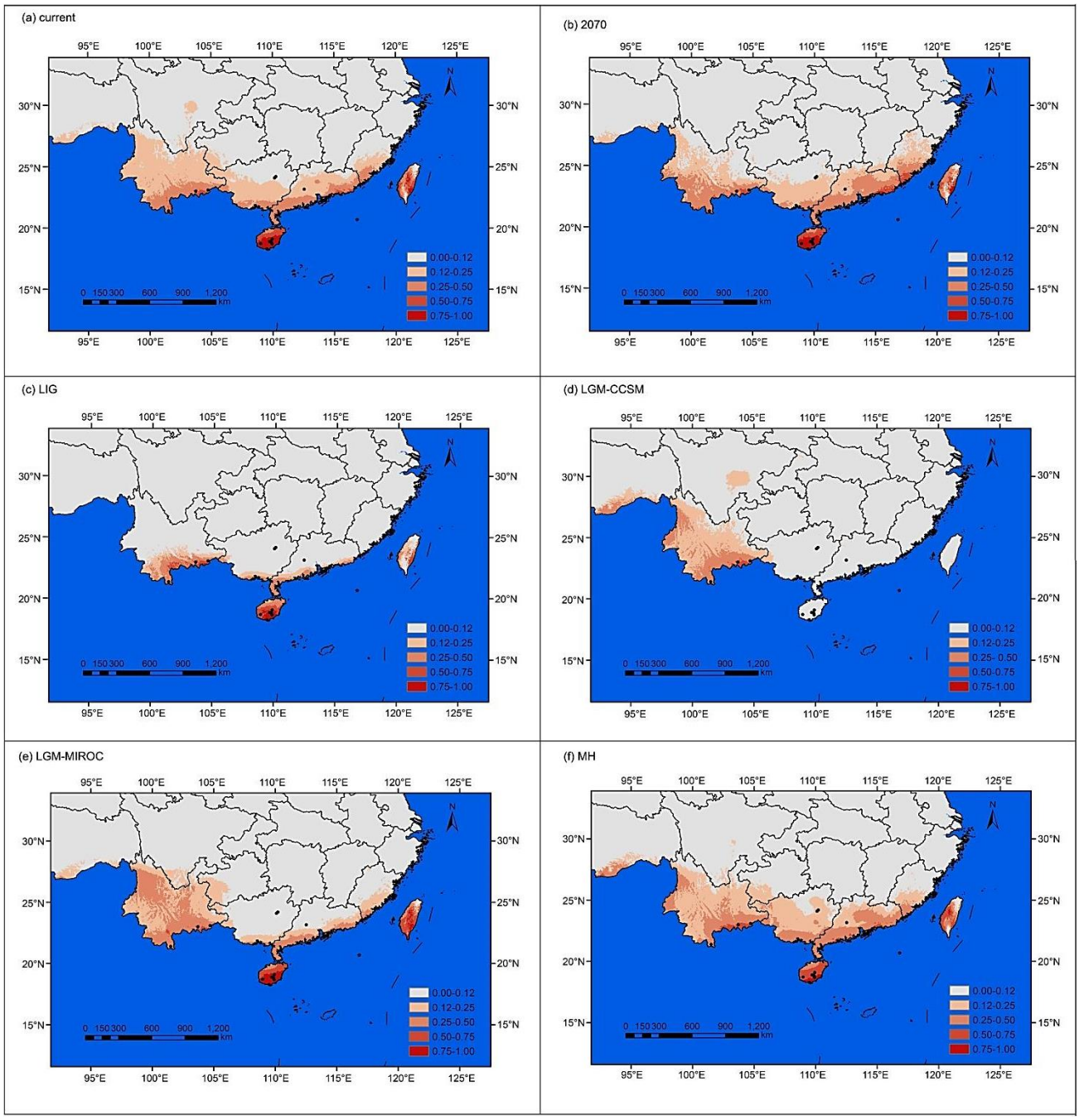

Fig. 11. The simulated distribution map of *Dacrycarpus imbricatus* during different period. (a) current conditions (1950-2000); (b) 2070; (c) Last interglacial (LIG); (d) Last Glacial Maximum (LGM) under CCSM model; (e) Last Glacial Maximum (LGM) under MIROC model; (f) Middle Holocene.

Discussion

This study demonstrates genetic diversity, population structure analyses, ecological niche modeling and phylogeographical pattern of *D. imbricatus* distributed in South China, based on the variability of *trnF-L* noncoding sequences of cpDNA.

Like the genetic variation obtained from coniferous plants (such as *P. koraiensis*, *Taxus cuspidata*, and *P. chiapensis*), the genetic variation within populations of *D. imbricatus* was greater than that between those populations (Tong *et al*., 2020; Su *et al*., 2018; Newton *et al*., 2002), which was consistent with the conclusion that the genetic variation of perennial outcrossing long-lived gymnosperms mainly existed within the population (Hamrick & Godt, 1989). The gene differentiation coefficient of *D. imbricatus* was 0.08755, the migration number was 2.61, and the genetic differentiation was 0.10388, implying that the genetic differentiation of the population was moderate. Biological characteristics such as heterotypic reproductive system, long-range dispersal of seeds, abundant wind-pollination, and long life (Proctor & Yeo, 1973; Fu & Jin, 1992; Enright & Ogden, 1995; Fu *et al*., 1999) were reduced and thus prevented differences between populations (Allnutt *et al*., 1999; Su *et al*., 2010). In addition, ecological and living characteristics had some impact on the differentiation of the *D. imbricatus* populations (Su *et al*., 2010). Like

Coniferopsida, *D. imbricatus* is wind-pollinated, and a large amount of pollen flow affects the genetic structure and spatial pattern of chloroplast markers. Moreover, with a long evolutionary history, different habitats may have different selection pressures. Very many variations have accumulated in its long evolutionary history (Huang *et al*., 2001), and private haplotypes have formed in different populations. The population haplotype diversity and nucleotide diversity are at a moderate level (*Hd* = 0.719; $\pi = 1.63 \times 10^{-3}$), lower than for *Cycas taitungensis* (*Hd* = 0.998; $\pi = 1.27 \times 10^{-2}$) (Huang *et al*., 2001), *Abies chensiensis* (*Hd* = 0.820; $\pi = 2.07 \times 10^{-3}$) (Shao *et al*., 2017) and *A. spinulosa* (*Hd* = 0.929; $\pi = 2.23 \times 10^{-2}$) (Su *et al*., 2005), but higher than for *A. recurvata* (*Hd* = 0.376; $\pi = 7.2 \times 10^{-4}$) (Shao & Xiang, 2015), *Tsuga forrestii* (*Hd* = 0.663; $\pi = 3.6 \times 10^{-4}$) (Cun & Wang, 2015) and *Ephedra saxatilis* (*Hd* = 0.258; $\pi = 2.52 \times 10^{-4}$) (Qin *et al*., 2013). The haplotype network diagram indicates that the haplotype exchanges between Guangdong province and Hainan Island were frequent. For example, haplotype H17 (Guangdong) was derived from H7 (Hainan Island), and haplotype H12 (Hainan Island) from H21 (Guangdong) (Fig. 4). This has been thought to be related to the land bridge that appeared in the ice age (Xu *et al*., 2010). In addition, the haplotype and nucleotide diversities of DH and NS in mainland populations were significantly higher than those of JFL, BWL, and WZ in the island populations. Due to the founder effect and limited effective population size, the genetic variation of island populations is generally lower than that of continental populations. This study further demonstrated that even when the island populations were larger than those of the mainland, the mainland populations still maintained higher genetic variation. Furthermore, because of the different ecological environments of mainland and islands, different populations might experience different selection pressures (Kimura & Weiss, 1964; Nielsen, 2004; Su *et al*., 2010). Therefore, different populations gave rise to different haplotypes.

Ecological niche modeling illustrated that the distribution range of the *D. imbricatus* population expanded northward gradually (Fig. 11), which was perhaps closely related to climate warming. In North America, pollen analysis showed that tree populations moved northward in response to postglacial warming (Davis, 1981; Nogués-Bravo *et al*., 2010). The degree of genetic differentiation between the Yunnan population (NS) and the Hainan Island populations (WZ, JFL, BWL, and DLS) was significant. It indicates that there was a barrier between NS and the other populations, revealing that geographic distance served as a crucial factor in population genetic structure (Liu *et al*., 2020). *D. imbricatus* was widely distributed with sample locations as far as 1,227,618 meters apart (between the NS and DH populations). Moreover, the widely distributed species tended to have high genetic diversity (Gitzendanner & Soltis, 2000, Maki *et al*., 2002, Su *et al*., 2009). As the overall size of the *D. imbricatus* population was large, and the longevity of plants was conducive to maintaining high genetic variation (Varvio *et al*., 1986, Maki & Morita, 1998), the NS population had high genetic diversity. Bayesian skyline plot indicated that the effective population size declined slowly from 35 to 5 Ma, then rose sharply from 2.5 Ma to the present. During the mid-Pleistocene (~1.0 to 0.78 Ma), the warm and humid East Asian summer monsoon intensified (Zhang & Liu, 2010; Ao *et al*., 2012; Han *et al*., 2003; Qi *et al*., 2014). Affected by subtropical and tropical monsoon climates, southern China had abundant rainfall, humid air, and high plant diversity (Qian & Ricklefs, 2000). The warm and humid climate is thought to have promoted the expansion of the habitat of *D. imbricatus* and increased its effective population.

The haplotype phylogeny of *D. imbricatus* on mainland China and Hainan Island presented a mixed pattern, indicating that the Qiongzhou Strait did not serve as a geographic barrier between the South China and Hainan Island populations. Qiongzhou Strait formed about 25 to 2.5 Ma (Zhao *et al*., 2007; Sui *et al*., 2018). With the fluctuation of global climate, sea level rose and fell periodically (Zhao *et al*., 2007), with a final formation time about 7,000 to 11,000 years ago (Sui *et al*., 2018; Zhao *et al*., 2007; Ni *et al*., 2014). During that ice age, the sea level fell and a land bridge formed between mainland China and Hainan Island. The appearance of the land bridge provided a means for the migration and diffusion of species and promoted secondary contact and gene exchange between the *D. imbricatus* populations on both sides of the Qiongzhou Strait (Jowers *et al*., 2015; Xu *et al*., 2010). In the Middle Pleistocene, land bridges were formed three times, from 0.6 to 0.8 Ma, 0.42 to 0.48 Ma, and 0.13 to 0.3 Ma, respectively (Shi *et al*., 2006; Huang *et al*., 2013). During interglacial periods, the submergence of land bridges may have limited gene exchange between populations. Simultaneously, genetic differentiation promoted the adaption of the species to its ecological environments, which led to the differentiation of different haplotypes. In addition, the divergence time between different haplotypes of *D. imbricatus* was 21.01 Ma (95% HPD: 37.25 to 7.86 Ma) (Fig. 5), which was during the formation of Qiongzhou Strait. The inference is that Qiongzhou Strait had a practical impact on the genetic structure of *D. imbricatus* on mainland China and Hainan Island but was not an effective biogeographic barrier. These results contribute to a better understanding of the geographical events imposed on gymnosperm in South China.

Conclusion

Phylogeography analysis may contribute to finding the potential distribution area of *D. imbricatus* and establishing appropriate management practices. The findings of this study indicated that there were many private haplotypes in different populations of *D. imbricatus* and no significant phylogeographic patterns between its island and the mainland populations. Qiongzhou Strait did not serve as a geographic barrier in genetic variation. In the process of restoring and protecting the species, focusing on local protection is suggested, especially by developing and establishing nature reserves to expand the range and scale of *D. imbricatus* populations.

Data availability

The *trnF-L* noncoding sequences of haplotypes generated in current study are available in GenBank, https://www.ncbi.nlm.nih.gov/genbank/ (accession numbers are described in the text).

Acknowledgements

This work was supported by the National Natural Science Foundation of China [31670200, 31770587, 31872670, and 32071781], Guangdong Basic and Applied Basic Research Foundation [2021A1515010911], and Project of Department of Science and Technology of Shenzhen City, Guangdong, China [JCYJ2019081317200 1780 and JCYJ20210324141000001].

References

Allnutt, T.R., A.C. Newton, A. Lara, A. Premoli, J.J. Armesto, R. Vergara and M. Gardner. 1999. Gardner Genetic variation in *Fitzroya cupressoides* (alerce), a threatened South American conifer. *Mol. Ecol*., 8: 975-987.

Ao, H., M.J. Dekkers, G. Xiao, X. Yang, L. Qin, X. Liu, X. Qiang, H. Chang and H. Zhao. 2012. Different orbital rhythms in the Asian summer monsoon records from North and South China during the Pleistocene. *Global Planet Chang.*, 80: 51-60.

Bai, P., J. Yang, L. Xie, S. Zhang and Z. Ling. 2020. Effect of topography on the cold water region in the east entrance area of Qiongzhou Strait. *Estuar Coast Shelf Sci.*, 242: 106820.

Chen, C., P. Li, M. Shi, J. Zuo, M. Chen and H. Sun. 2009. Numerical study of the tides and residual currents in the Qiongzhou Strait. *Chin. J. Oceanol. Limnol.*, 27: 931-942.

Chen, D., X. Zhang, H. Kang, X. Sun, S. Yin, H. Du, N. Yamanaka, W. Gapare, H.X. Wu and C. Liu. 2012. Phylogeography of *Quercus variabilis* based on chloroplast DNA sequence in East Asia: multiple glacial refugia and mainland-migrated island populations. *PLoS One*, 7: e47268.

Chiang, Y.C., K.H. Hung, B.A. Schaal, X.J. Ge, T.W. Hsu and T.Y. Chiang. 2006. Contrasting phylogeographical patterns between mainland and island taxa of the *Pinus luchuensis* complex. *Mol. Ecol.*, 15: 765-779.

Collins, W.D., C.M. Bitz, M.L. Blackmon, G.B. Bonan, C.S. Bretherton, J.A. Carton, P. Chang, S.C. Doney, J.J. Hack, T.B. Henderson, J.T. Kiehl, W.G. Large, D.S. McKenna, B.D. Santer and R.D. Smith. 2006. The Community Climate System Model version 3 (CCSM3). *J. Climate*, 19: 2122-2143.

Cornuet, J.M., P. Pudlo, J. Veyssier, A. Dehne-Garcia, M. Gautier, R. Leblois, J.M. Marin and A. Estoup. 2014. DIYABC v20: a software to make approximate Bayesian computation inferences about population history using single nucleotide polymorphism DNA sequence and microsatellite data. *Bioinformatics*, 30: 1187-1189.

Cun, Y.Z. and X.Q. Wang. 2015. Phylogeography and evolution of three closely related species of *Tsuga* (hemlock) from subtropical eastern Asia: Further insights into speciation of conifers. *J. Biogeography*, 42: 315-327.

Darriba, D., G.L. Taboada, R. Doallo and D. Posada. 2012. jModelTest 2: more models new heuristics and parallel computing. *Nat. Methods*, 9: 772.

Davis, M.B. 1981. Quaternary history and the stability of forest communities. In: (Eds.): West, D.C., H.H. Shugart and D.B. Botkin *Forest succession: concepts and application*. Springer-Verlag, Berlin, pp. 132-153.

de Laubenfels, D.J. 1988. Coniferales. In: (Eds.): Van Steenis, C.G.G.J. and W.J.J.O. De Wilde. *Flora Malesiana*, vol 10. Noordhoff International Publishing Leyden, pp. 337-453.

Drummond, A.J., A. Rambaut, B. Shapiro and O.G. Pybus. 2005. Bayesian coalescent inference of past population dynamics from molecular sequences. *Mol. Biol. Evol*., 22: 1185-1192.

Drummond, A.J., M.A. Suchard, D. Xie and A. Rambaut. 2012. Bayesian phylogenetics with BEAUti and the BEAST 1.7. *Mol. Biol. Evol.,* 29: 1969-1973.

Enright, N.J. and J. Ogden. 1995. The southern conifers-a synthesis. In: (Eds.): Enright, N.J. and R.S. Hill. *Ecology of the Southern Conifers*. Melbourne University Press, Victoria, pp. 271-287.

Excoffier, L. and H.E.L. Lischer. 2010. Arlequin suite ver 35: a new series of programs to perform population genetics analyses under Linux and Windows. *Mol. Ecol. Resour.*, 10: 564-567.

Fawcett, T. 2006. An introduction to ROC analysis. *Pattern Recogn. Lett.,* 27: 861-874.

Felsenstein, J. 1989. PHYLIP-phylogeny inference package (version 32). *Cladistics*, 5: 164-166.

Fu, L.G. and J.M. Jin (Eds.). 1992. *Red List of Endangered Plants in China*, vol 1. Science Press, Beijing.

Fu, L.G., Y. Li and R.R. Mill. 1999. Podocarpaceae. In: (Eds.): Wu, Z. and P.H. Raven. *Flora of China. Cycadaceae Through Fagaceae, vol 4*. Science Press, Beijing/ Missouri Botanical Garden Press, St. Louis, pp. 78-84.

Fu, Y.X. and W.H. Li. 1993. Statistical tests of neutrality of mutations. *Genetics*, 133: 693-709.

Gitzendanner. M.A. and P.S. Soltis. 2000. Patterns of genetic variation in rare and widespread plant congeners. *Amer. J. Bot.,* 87: 783-792.

Hall, T.A. 1999. BioEdit: a user-friendly biological sequence alignment editor and analysis program for Windows 95/98/NT. *Nucleic Acids Symp. Ser.*, 41: 95-98.

Hamrick, J.L. and M.J.W. Godt. 1989. Allozyme diversity in plant species. In: (Eds.): Brown, A.H.D., M.T. Clegg, A.L. Kahler and B.S. Weir. *Plant Population Genetics, Breeding and Germplasm Resources*. Sinauer Associates Sunderland, pp. 43-63.

Han, W.X., X.M. Fang and A. Berger. 2003. Tibet forcing of mid-Pleistocene synchronous enhancement of East Asian winter and summer monsoons revealed by Chinese loess record. *Quat. Res.*, 78: 174-184.

Harpending, H.C. 1994. Signature of ancient population growth in a low-resolution mitochondrial DNA mismatch distribution. *Hum. Biol.,* 66: 591-600.

Hasumi, H. and S. Emori. 2004. K-1 Coupled GCM (MIROC) description [K-1 Model Developers TechRep11-34]. In: (Eds.): Hasumi, H. and S. Emori. Center for Climate System Research, University of Tokyo, pp. 34.

Hewitt, G. 2000. The genetic legacy of the Quaternary ice ages. *Nature*, 405: 907-913.

Hewitt, G. 2004. Genetic consequences of climatic oscillations in the Quaternary. *Philos. Trans. R. Soc. Lond. B Biol. Sci.*, 359: 183-195.

Hill, R.S. and R.J. Carpenter. 1991. Evolution of *Acmopyle* and *Dacrycarpus* (Podocarpaceae) foliage as inferred from macrofossils in south-eastern Australia. *Aust. Syst. Bot.*, 4: 449-480.

Huang, S., Y.C. Chiang, B.A. Schaal and C.H. Chou. 2001. Organelle DNA phylogeography of *Cycas taitungensis* a relict species in Taiwan. *Mol. Ecol.*, 10: 2669-2681.

Huang, Y., X. Guo, S.Y.W. Ho, H. Shi, J. Li, J. Li, B. Cai and Y. Wang. 2013. Diversification and Demography of the Oriental Garden Lizard (*Calotes versicolor*) on Hainan Island and the Adjacent Mainland. *PLoS One*, 8: e64754.

Jaros, U., A. Tribsch and H.P. Comes. 2018. Diversification in continental island archipelagos: new evidence on the roles of fragmentation colonization and gene flow on the genetic divergence of *Aegean Nigella* (Ranunculaceae). *Ann. Bot. London*, 121: 241-254.

Jowers, M.J., R.M. Lehtinen, R.J. Downie, A.P. Georgiadis and J.C. Murphy. 2015. Molecular phylogenetics of the glass frog *Hyalinobatrachium orientale* (Anura: Centrolenidae): evidence for Pliocene connections between mainland Venezuela and the island of Tobago. *Mitochondrial DNA*, 26: 613-618.

Kimura, M. and G.H. Weiss. 1964. The stepping stone model of population structure and the decrease of genetic correlation with distance. *Genetics*, 49: 561-576.

Kissling, W.D., W.J. Baker, H. Balslev, F. Borchsenius, J. Dransfield, R. Govaerts and J.C. Svenning. 2012. Quaternary and pre-Quaternary historical legacies in the global distribution of a major tropical plant lineage. *Glob. Ecol. Biogeogr.,* 21: 909-921.

Kranitz, M.L., E. Biffin, A. Clark, M.L. Hollingsworth, M. Ruhsam, M.F. Gardner, P. Thomas, R.R. Mill, R.A. Ennos, M. Gaudeul, A.J. Lowe and P.M. Hollingsworth. 2014. Evolutionary diversification of new Caledonian Araucaria. *PLoS One*, 9(10): e110308.

Leng, X., Z. Wang, S. An, J. Feng, Y. Liu and G. Wang. 2005. ISSR analysis of genetic diversity of *Ilex integra* an insular endemic plant. *Biodiv. Sci.*, 13: 546-554.

Li, J. 2019. The complete chloroplast genome sequence of *Podocarpus imbricatus* (Podocarpaceae) and its phylogenetic analysis. *Mitochondrial DNA B Resour.*, 4: 368-369.

Librado, P. and J. Rozas. 2009. DnaSP v5: a software for comprehensive analysis of DNA polymorphism data. *Bioinformatics*, 25: 1451-1452.

Liu, Y., H.T. Pham, Z. He and C. Wei. 2020. Phylogeography of the cicada *Platypleura hilpa* in subtropical and tropical East Asia based on mitochondrial and nuclear genes and microsatellite markers. *Int. J. Biol. Macromol.*, 151: 529-544.

Maki, M., S. Horie and J. Yokoyama. 2002. Comparison of genetic diversity between narrowly endemic shrub *Menziesia goyozanensis* and its widespread congener *M. pentandra* (Ericaceae). *Consmot. Genet.*, 3: 421-425.

Maki, M. and H. Morita. 1998. Genetic diversity in island and mainland populations of *Aster spathulifolius* (Asteraceae). *Int. J. Plant Sci.,* 159: 148-152.

Manni, F., E. Guérard and E. Heyer. 2004. Geographic patterns of (genetic morphologic linguistic) variation: how barriers can be detected by using "Monmonier's algorithm". *Hum. Biol.*, 76: 173-190.

Mantel, N. 1967. The detection of disease clustering and a generalized regression approach. *Cancer Res.,* 27: 209-220.

Nei, M. 1973. Analysis of gene diversity in subdivided populations. *Proc. Natl. Acad. Sci. USA.*, 70: 3321-3323.

Newton, A.C., T.R. Allnutt, W.S. Dvorak, R.F. Del Castillo and R.A. Ennos. 2002. Patterns of genetic variation in *Pinus chiapensis* a threatened Mexican pine detected by RAPD and mitochondrial DNA RFLP markers. *Heredity*, 89: 191-198.

Ni, Y., Z. Xia and S. Ma. 2014. The opening of Qiongzhou Strait: evidence from sub-bottom profiles. *Marine Geol. & Quat. Geol.*, 34: 79-82.

Nielsen, L.R. 2004. Molecular differentiation within and among island populations of the endemic plant *Scalesia affinis* (Asteraceae) from the Galápagos Islands. *Heredity*, 93: 434-442.

Nogués-Bravo, D., R. Ohlemüller, P. Batra and M.B. Araújo. 2010. Climate predictors of late Quaternary extinctions. *Evolution*, 64: 2442-2449.

Parker, M.A., W. Malek and I.M. Parker. 2006. Growth of an invasive legume is symbiont limited in newly occupied habitats. *Divers. Distrib.*, 12: 563-571.

Phillips, S.J., R.P. Anderson and R.E. Schapire. 2006. Maximum entropy modeling of species geographic distributions. *Ecol. Model*, 190: 231-259.

Proctor, M. and P. Yeo (Eds.). 1973. The Pollination of Flowers Collins, London.

Qi, X.S., N. Yuan, H.P. Comes, S. Sakaguchi and Y.X. Qiu. 2014. A strong 'filter' effect of the East China Sea land bridge for East Asia's temperate plant species: inferences from molecular phylogeography and ecological niche modelling of *Platycrater arguta* (Hydrangeaceae). *B.M.C. Evol. Biol.*, 14: 41.

Qian, H. and R.E. Ricklefs. 2000. Large-scale processes and the Asian bias in species diversity of temperate plants. *Nature*, 407: 180-182.

Qin, A.L., M.M. Wang, Y.Z. Cun, F.S. Yang, S.S. Wang, J.H. Ran and X.Q. Wang. 2013. Phylogeographic evidence for a link of species divergence of Ephedra in the Qinghai-Tibetan Plateau and adjacent regions to the Miocene Asian aridification. *PLoS One*, 8(2): e56243.

Quiroga, M.P., P. Mathiasen, A. Iglesias, R.R. Mill and A.C. Premoli. 2016. Molecular and fossil evidence disentangle the biogeographical history of *Podocarpus* a key genus in plant geography. *J. Biogeogr.*, 43: 372-383.

Shao, Y.Z. and Q.P. Xiang. 2015. Species delimitation and phylogeography of the *Abies chensiensis* complex inferred from morphological and molecular data. *Bot. J. Linn. Soc.*, 177: 175-188.

Shao, Y.Z., X.C. Zhang, L.K. Phan and Q.P. Xiang. 2017. Elevation shift in *Abies* Mill (Pinaceae) of subtropical and temperate China and Vietnam-corroborative evidence from cytoplasmic DNA and ecological niche modelling. *Front. Plant Sci.*, 8: 578.

Shi, M., C. Chen, Q. Xu, H. Lin, G. Liu, H. Wang, F. Wang and J. Yan. 2002. The role of Qiongzhou Strait in the seasonal variation of the South China sea circulation. *J. Phys. Oceanogr.,* 32: 103-121.

Shi, Y.F., Z.J. Cui and Z. Su (Eds.). 2006. The Quaternary Glaciations and Environmental Variations in China. Shijiazhuang: Hebei Science and Technology Press.

Su, J., Y. Yan, J. Song, J. Li, J. Mao, N. Wang, W. Wang and F.K. Du. 2018. Recent fragmentation may not alter genetic patterns in endangered long-lived species: evidence from *Taxus cuspidate*. *Front. Plant Sci.*, 9: 1571.

Su, Y.J., T. Wang and F. Deng. 2010. Contrasting genetic variation and differentiation on Hainan Island and the Chinese mainland populations of *Dacrycarpus imbricatus* (Podocarpaceae). *Biochem. Syst. Ecol.,* 38: 576-584.

Su, Y.J., T. Wang and P. Ouyang. 2009. High genetic differentiation and variation as revealed by ISSR marker in *Pseudotaxus chienii* (Taxaceae) an old rare conifer endemic to China. *Biochem. Syst. Ecol*., 37: 579-588.

Su, Y.J., T. Wang, B. Zheng, Y. Jiang, G.P. Chen, P.Y. Ouyang and Y.F. Sun. 2005. Genetic differentiation of relictual populations of *Alsophila spinulosa* in southern China inferred from cpDNA *trnL-F* noncoding sequences. *Mol. Phylogenet. Evol*., 34: 323-333.

Sui, Y., L. Zhang, X.D. Mu, Z.Y. Wang, T. Li, H. Wang and J.N. Zhen. 2018. Coastline change detection and analysis with remote sensing in Hainan Island. *J. Marine Sci.*, 36: 36-43.

Swets, J.A. 1988. Measuring the accuracy of diagnostic systems. *Science*, 240: 1285-1293.

Taberlet, P., L. Gielly, G. Pautou and J. Bouvet. 1991. Universal primers for amplification of three non-coding regions of chloroplast DNA. *Plant Mol. Biol.*, 17: 1105-1109.

Tajima, F. 1989. Statistical-method for testing the neutral mutation hypothesis by DNA polymorphism. *Genetics*, 123: 585-595.

Thomas, P., K. Sengdala, V. Lamxay and E. Khou. 2007. New records of conifers in Cambodia and Laos. *Edinb. J. Bot.*, 64: 1-9.

Tong, Y.W., B.J. Lewis, W.M. Zhou, C.R. Mao, Y. Wang, L. Zhou, D.P. Yu, L.M. Dai and L. Qi. 2020. Genetic diversity and population structure of natural *Pinus koraiensis* populations. *Forests,* 11: 39.

Varvio, S.L., R. Chakraborty and M. Nei. 1986. Genetic variation in subdivided populations and conservation genetics. *Heredity*, 57: 189-198.

Wallace, L.E., G.L. Wheeler, M.E. McGlaughlin, G. Bresowar and K. Helenurm. 2017. Phylogeography and genetic structure of endemic *Acmispon argophyllus* and *A dendroideus* (Fabaceae) across the California Channel Islands. *Amer. J. Bot*., 104: 743-756.

Wilf, P. 2012. Rainforest conifers of Eocene Patagonia: Attached cones and foliage of the extant Southeast Asian and Australasian genus *Dacrycarpus* (Podocarpaceae). *Amer. J. Bot.,* 99: 562-584.

Xu, L., C. He, C. Shen, T. Jiang, L. Shi, K. Sun, S.W. Berquist and J. Feng. 2010. Phylogeography and population genetic structure of the great leaf-nosed bat (*Hipposideros armiger*) in China. *J. Hered.,* 101: 562-572.

Yu, Y., A.J. Harris, C. Blair and X. He. 2015. RASP (Reconstruct Ancestral State in Phylogenies): a tool for historical biogeography. *Mol. Phylogenet. Evol*., 87: 46-49.

Zhang, R. and X.D. Liu. 2010. The effects of tectonic uplift on the evolution of Asian summer monsoon climate since Pliocene. *Chinese J. Geophys.*, 53: 948-960.

Zhao, H., L. Wang and J. Yuan. 2007. Origin and time of Qiongzhou Strait (in Chinese). *Marine Geology and Quaternary Geology*, 27: 33-40.

Zhou, Q.X. and Z.J. Gu. 2001. Karyomorphology of *Podocarpus* sl in China and its systematic significance. *Caryologia -Firenze-*, 54: 121-127.

Zhu, X.H., Y.L. Ma, X. Guo, X. Fan, Y. Long, Y. Yuan, J.L. Xuan and D. Huang. 2014. Tidal and residual currents in the Qiongzhou Strait estimated from shipboard ADCP data using a modified tidal harmonic analysis method. *J. Geophys. Res. Oceans*, 119: 8039-8060.

(Received for publication 21 June 2021)